crystals

MDPI

Article

Optimization of Enzyme-Mediated Calcite Precipitation as a Soil-Improvement Technique: The Effect of Aragonite and Gypsum on the Mechanical Properties of Treated Sand

Heriansyah Putra [1,2,*], Hideaki Yasuhara [3], Naoki Kinoshita [3] and Akira Hirata [4]

1 Graduate School Science and Engineering, Ehime University, Matsuyama 790-8577, Japan
2 Faculty of Engineering, Universitas Jambi, Jambi 36361, Indonesia
3 Department of Civil and Environmental Engineering, Ehime University, Matsuyama 790-8577, Japan; hide@cee.ehime-u.ac.jp (H.Y.); kino@cee.ehime-u.ac.jp (N.K.)
4 Department of Applied Chemistry, Ehime University, Matsuyama 790-8577, Japan; ahirata@ehime-u.ac.jp
* Correspondence: putra.heriansyah@cee.ehime-u.ac.jp; Tel.: +81-90-7570-8283

Academic Editor: Helmut Cölfen
Received: 12 December 2016; Accepted: 17 February 2017; Published: 20 February 2017

Abstract: The effectiveness of magnesium as a substitute material in enzyme-mediated calcite precipitation was evaluated. Magnesium sulfate was added to the injecting solution composed of urea, urease, and calcium chloride. The effect of the substitution on the amount of precipitated materials was evaluated through precipitation tests. X-ray powder diffraction and scanning electron microscopy analyses were conducted to examine the mineralogical morphology of the precipitated minerals and to determine the effect of magnesium on the composition of the precipitated materials. In addition to calcite, aragonite and gypsum were formed as the precipitated materials. The effect of the presence of aragonite and gypsum, in addition to calcite, as a soil-improvement technique was evaluated through unconfined compressive strength tests. Soil specimens were prepared in polyvinyl chloride cylinders and treated with concentration-controlled solutions, which produced calcite, aragonite, and gypsum. The mineralogical analysis revealed that the low and high concentrations of magnesium sulfate effectively promoted the formation of aragonite and gypsum, respectively. The injecting solutions which produced aragonite and calcite brought about a significant improvement in soil strength. The presence of the precipitated materials, comprising 10% of the soil mass within a treated sand, generated a strength of 0.6 MPa.

Keywords: EMCP technique; calcite; aragonite; gypsum; grouting technique; soil improvement

1. Introduction

The calcite-induced precipitation method (CIPM) has been confirmed as a potential soil-improvement technique. It can significantly improve the engineering properties of soil, such as shear strength and stiffness [1–7] and can reduce the permeability [5,8–11]. Many of the studies have used bacterial cells, e.g., *Sporosarcina pasteurii*, to dissociate urea into ammonium and carbonate ions [5,7,12]. The produced carbonate ions are precipitated as calcite crystals in the presence of calcium ions. The reactions of the urea hydrolysis and the calcite formation are shown in Equations (1)–(3):

$$CO(NH_2)_2 + 2H_2O \rightarrow 2NH_4^+ + CO_3^{2-} \quad (1)$$

$$CaCl_2 \rightarrow Ca^{2+} + 2Cl^- \quad (2)$$

$$Ca^{2+} + CO_3^{2-} \rightarrow CaCO_3 \downarrow (\text{precipitated}) \quad (3)$$

In this technique, the grouting solution, which produces calcium carbonate (i.e., calcite, aragonite, and/or vaterite), is injected into the sand sample. The mixed solution of reagents composed of urea and $CaCl_2$ and a bio-catalytic agent (e.g., bacterial cell) is used as the grouting solution. The precipitated calcium carbonate in sandy soil may provide bridges between the grains of sand, restricting their movement and, thus, improving the strength and stiffness of the soil. The deposited calcite fills the voids, thereby reducing the permeability and porosity [8,9]. There are some complexities related to the use of bacteria in the calcite precipitation technique. For example, the bacterial incubation may be difficult to control because special treatments are required [13]. In addition, the high concentration of reagents may have an inhibitory effect on the growth rate of bacteria [14] and, hence, the bacterial activity may be limited in fine-grained soil [15,16]. An alternative methodology among calcite precipitation techniques, which is called enzyme-mediated calcite precipitation (EMCP) has been introduced in our previous works [1,2,4,9,13]. In this technique, the enzyme itself is used to dissociate urea into ammonium and carbonate ions instead of bacteria. Using an enzyme is more straightforward than using bacteria because biological treatments do not need to be considered [9]. Enzyme-reagent mixed solutions, which produce the precipitated calcite, are injected into soil specimens. Thus, unlike the CIPM procedure, the fixation of the enzyme is not required [9,13]. The efficacy of the EMCP technique has already been evaluated in previous works [1,4,9,10,13]. Levels of unconfined compressive strength, ranging from 400 kPa to 1.6 MPa, were achieved, and the permeability of the improved samples was reduced by more than one order of magnitude [9].

As for the grouting method, calcite precipitation techniques require many injection wells for treating the large volume [5]. A high amount of calcite is needed to improve the strength of porous media. Whiffin et al. [7] reported that 60 kg of precipitated materials should be precipitated in 1 m^3 of soil in order to obtain a sufficient strength of 300 kPa. This corresponds to precipitated materials comprising approximately 4% of the soil mass in the treated sand [7]. However, highly concentrated urea and $CaCl_2$ (>0.5 mol/L) decrease the efficiency of calcite precipitation [10,13,17]. Urea and $CaCl_2$, with concentrations of 0.05–0.50 mol/L, were reported to be the most efficient in the application of calcite precipitation techniques [13,17,18]. A high amount of precipitated materials has to be produced by a limited number of injections [5] and, hence, the efficiency of calcite precipitation in high concentrations of urea and $CaCl_2$ has to be improved.

Putra et al. [4] reported that the substitution of a low concentration of magnesium chloride may be able to improve the efficiency of the calcite precipitation technique. Precipitated materials comprising 90% of the maximum theoretical mass were obtained by substituting magnesium for 20% of the $CaCl_2$ solutions of 0.5 mol/L. However, as the concentration of magnesium was increased, the amount of precipitated material gradually decreased. The presence of magnesium in the calcite precipitation process, which has pH < 11, also has the potential to promote aragonite in addition to calcite [19]. Magnesium ions are found to be the most efficient ions for the aragonite synthesis [20]. Aragonite has a high mechanical strength and is regarded as a mineral which can improve the bending strength of rubber and plastics as a filler [20,21]. Despite a metastable relative to calcite, aragonite has higher Mohs hardness than calcite, namely, 3.25–4.00 and 3.00, respectively [22,23].In addition, the other calcium carbonate polymorph of vaterite may also be promoted during the precipitation process. Vaterite is an essential constituent of Portland cement and was found during oil field drilling [24]. As the calcium carbonate polymorph, aragonite and vaterite have the similar XRD patterns [25–28]. However, studies on the effects of aragonite on soil-improvement techniques have not been carried out yet.

In this work, magnesium sulfate was added as the substitute material in the enzyme-mediated calcite precipitation technique (EMCP), and its effects on the amount and the mineralogical substance of the precipitated materials were evaluated. Magnesium sulfate was added to the injecting solution to promote the formation of aragonite and gypsum in addition to calcite. The reactions of the gypsum formation are shown in Equations (4) and (5):

$$MgSO_4 \rightarrow Mg^{2+} + SO_4^{2-} \quad (4)$$

$$Ca^{2+} + SO_4^{2-} \rightarrow CaSO_4 \downarrow (\text{precipitated}) \quad (5)$$

The microstructures of the precipitated materials were examined by X-ray powder diffraction (XRD) and scanning electron microscopy (SEM) to observe the effects of magnesium on the phase and the substance of the precipitated materials. The effects of the presence of aragonite and gypsum in EMCP, as a soil-improvement technique, were examined through unconfined compressive strength (UCS) tests. The selected combinations for the grouting solution were fixed by precipitation tests and the mineralogical analyses, and then they were utilized to improve the strength of sand specimens. Soil specimens were prepared in polyvinyl chloride (PVC) cylinders and treated with concentration-controlled solutions composed of urea, urease, calcium chloride, and magnesium sulfate. Finally, by comparing the relation between the numbers of injections, the mineral mass, and the UCS within the treated specimens obtained in this study, with those obtained from the literature, the influence of the aragonite and/or the gypsum minerals was explicitly investigated.

2. Materials and Methods

2.1. Materials

The mixed solution of reagents composed of urea ($CO(NH_2)_2$), calcium chloride ($CaCl_2$), and magnesium sulfate ($MgSO_4$) and purified urease were used as the grouting material in this study. The high-purity reagents of urea, $CaCl_2$, and $MgSO_4$ were obtained from Kanto Chemicals Co., Inc., Tokyo, Japan. The urease enzyme (020-83242), purified from jack bean meal and with the activity of 2950 U/g, was used as the biocatalytic dissociation of urea. Silica sand #6 with e_{max}, e_{min}, coefficient of uniformity (CU), and specific gravities (Gs) of 0.899, 0.549, 1.550, and 2.653, respectively, was prepared to evaluate the effects of precipitated materials on the mechanical properties. It was classified as poorly-graded sand (SP) based on the unified soil classification system (USCS) [29]. The grain size distribution curve of silica sand #6 is shown in Figure 1 [4,30].

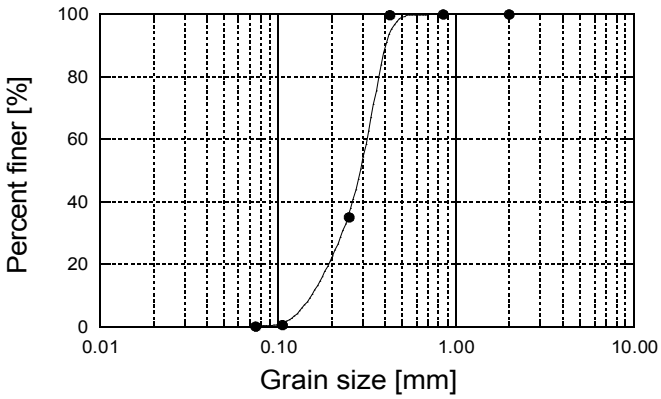

Figure 1. Particle size distribution of silica sand #6 used in this work [4,30].

2.2. Precipitation Tests

Precipitation tests were performed directly in transparent test tubes to evaluate the amount of precipitated materials. The experimental procedures developed by Neupane et al. [13] and Putra et al. [4] were adopted in this work. Urease with concentrations of 1.0, 2.0, 3.0, 4.0, and 5.0 g/L and distilled water were mixed separately. The mixed solutions were stirred for 2 min and then filtered through filter paper (pore size (PS) of 11 μm) to remove the undissolved particles. The particles retained on the filter paper were dried at 60 °C for 24 h, and then the amount of solved particles was evaluated. The solved particles were shown as a percentage, namely, the ratio of the solved mass to the mixed mass of urease. The urea and $CaCl_2$, with a concentration of 1.0 mol/L, were mixed with distilled water. The filtered urease and urea-$CaCl_2$ solutions were mixed thoroughly in a transparent

test tube, to obtain a total volume of 30 mL, and then allowed to react for an entire three-day curing period. Samples were kept in a box without shaking at a room temperature of 20 °C. After the curing time, the grouting solution was filtered through filter paper (PS of 11 μm). The particles retained on the filter paper and the particles remaining in the tubes were dried at 60 °C for 24 h, and then the total mass of the precipitated minerals was evaluated by combining the precipitated minerals deposited in the test tubes with the materials remaining on the filter paper. Two identical tests were conducted for each condition to check the reproducibility. The mass of the precipitated minerals was shown as the precipitation ratio, namely, the ratio of the actual mass of the precipitated minerals to the theoretical mass of the maximum precipitation of $CaCO_3$ (Equations (6) and (7)):

$$\text{Precipitaion ratio } (\%) = \frac{\text{actual mass of precipitated minerals } (m_p)}{\text{theoretical mass of } CaCO_3 (m_t)} \quad (6)$$

$$m_t = C \times V \times M \quad (7)$$

where:

m_p: mass of the precipitated materials evaluated from the tests (g)
m_t: theoretical mass of $CaCO_3$ (g)
C: concentration of the solution (mol/L)
V: volume of the solution (L)
M: molar mass of $CaCO_3$ (100.087 g/mol)

The relation among the urease concentrations, the mass of solved particles, and the precipitation ratio was assessed to determine the optimum urease concentration.

Magnesium sulfate was newly-added to the grouting solution. The concentrations of magnesium sulfate, varying from 0.02 to 0.10 mol/L, were substituted to obtain a total concentration of $CaCl_2$–$MgSO_4$ of 1.0 mol/L. The selected concentration of urease was utilized to dissociate the 1.0 mol/L of urea. The effects of magnesium sulfate on the amount and the mineralogical substance of the precipitated materials were evaluated. The experimental conditions for the test tube experiments are listed in Table 1. The total amount of precipitated materials was examined thoroughly by the tests. The morphologies of the dried precipitated materials were characterized by XRD, and the evolutions of the shapes of the particles were observed by SEM.

Table 1. Experimental conditions for test tube experiments to evaluate the effect of magnesium.

Case	Conc. of Urea	Conc. of $CaCl_2$	Conc. of $MgSO_4$
	(mol/L)	(mol/L)	(mol/L)
A0	1.00	1.00	0.00
A1	1.00	0.98	0.02
A2	1.00	0.96	0.04
A3	1.00	0.94	0.06
A4	1.00	0.92	0.08
A5	1.00	0.90	0.10

2.3. Mineralogical Analysis

XRD patterns were recorded on a Rigaku RINT2200, Tokyo, Japan using a scanning 2θ range from 2°–50°. The dried precipitated materials were observed to evaluate the effect of the substitution of magnesium sulfate on the mineralogical substance of precipitated materials. An XRD quantitative analysis was used to obtain the mineral composition of the precipitated materials [31–33]. The procedure was as follows: The mineral types of the precipitated materials were obtained from the XRD analysis. The pure minerals for each mineral of the precipitated materials and internal

standard material were prepared to develop the calibration curve. They can be determined after the precipitated materials have been identified by the XRD analysis. The internal standard materials should have a simple pattern and peaks that do not overlap with the peaks of the targeted materials [33]. The calibration curve was developed by mixing the pure and the internal standard materials with ratios of 0%–100%, 10%–90%, 30%–70%, 50%–50%, 70%–30%, 90%–10%, and 100%–0%, respectively. The fixed mass of the pure minerals was taken in a porcelain basin and mixed with the internal standard materials. The XRD analysis was conducted on the mixed materials, and the intensity of the main peak of the pure materials was examined. The same procedure was adopted for the different proportions of pure and internal standard materials and, consequently, the calibration curve could be drawn.

In order to eliminate any errors during the sample preparation, validation data were also provided. The fixed mass of pure materials was mixed at different ratios, without the internal standard materials, and was prepared for the XRD analysis with the same procedure. The intensity of the main peak of the materials was plotted on the calibration curve, and the mass of the materials was examined. The error was shown as a percentage error, namely, the ratio of the difference in mass between the mass of the mixed materials and the obtained mass from the calibration curve to the mass of the mixed materials.

2.4. Unconfined Compressive Strength Tests

Unconfined compressive strength (UCS) tests were conducted to evaluate the improvement in mechanical properties of the treated sand specimens. Polyvinyl chloride (PVC) cylinders, 5 cm in diameter and 10 cm in height, were used to prepare the sand specimens. The fixed volume of the grouting solution was injected into the prepared sand specimens. The injected volume was controlled by the number of pore volumes (PV), one PV being ~75 mL. Firstly, dry silica sand with a relative density of 50% was prepared in the PVC cylinders. Secondly, one PV of the grout solution was poured into the PVC cylinders from the top. The sand samples were treated by 1–3 PV with a three-day curing time. After the curing time, the treated sand was removed from the PVC cylinders. The surface of the samples was flattened before the UCS tests were performed. The procedure of sample preparation for UCS tests is shown in Figure 2. Two tests were carried out for each condition to check the reproducibility. The UCS tests were performed under wet conditions to avoid any unexpected precipitation that may occur when specimens are intentionally dried out.

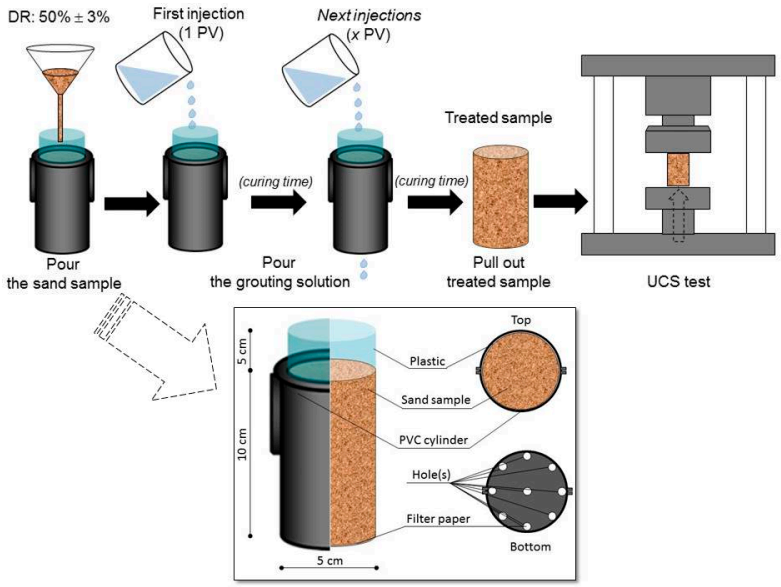

Figure 2. Procedure of sample preparation for UCS test.

3. Results and Discussion

The efficiency of varying the concentrations of urease on the calcite precipitation technique was evaluated. Figure 3 shows the relation among the urease concentration, the solved mass of urease, and the precipitation ratio of the calcite. It should be noticed that the reproducibility of the two identical tests under each experimental condition was confirmed. As is apparent, the precipitated ratio increased significantly when 2.0 g/L of urease was added. The increase in the precipitated mass occurred due to the increase in the solved mass of urease in the grouting solution. However, the increasing urease concentration had no significant impact on the solved mass and, hence, there was no significant increase in the precipitated mass as the concentration was greater than 2.0 g/L. In the filtered process, when the mixed solution which was composed of a high concentration of urease was filtered, a high amount of undissolved urease remained on the filter paper and, hence, the filtered process was inefficient. The results indicated that the urease concentration in the filtered process was limited. Urease with a concentration of 2.0 g/L was selected as the optimum concentration with the average consumed urease of 74% and precipitation ratio of 57%.

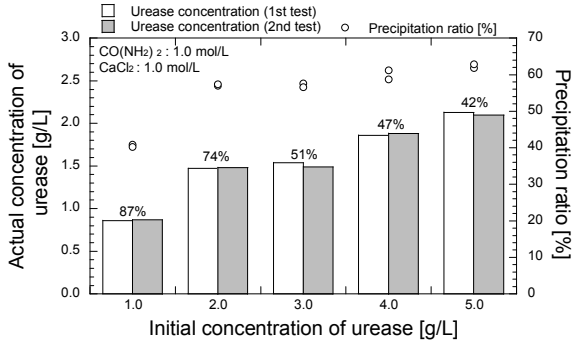

Figure 3. Evaluation of consumed urease and its effect on the precipitated ratio.

The effects of the substituted magnesium sulfate in the $CaCl_2$–urea solutions were evaluated. Filtered urease, with a concentration of 2.0 g/L, was mixed with various combinations of $CaCl_2$–$MgSO_4$ and 1.0 mol/L of urea. The evolutions of the precipitated mass, as the effect of the substitution of magnesium sulfate, are depicted in Figure 4. As is apparent, the precipitated amount gradually increased as the concentration of $MgSO_4$ was increased. A precipitation ratio of more than 100% was obtained when 0.10 mol/L of $MgSO_4$ was added. The results indicated that minerals other than calcite were formed during the precipitation process. Therefore, a mineralogical analysis was needed to determine the type and the composition of the precipitated materials.

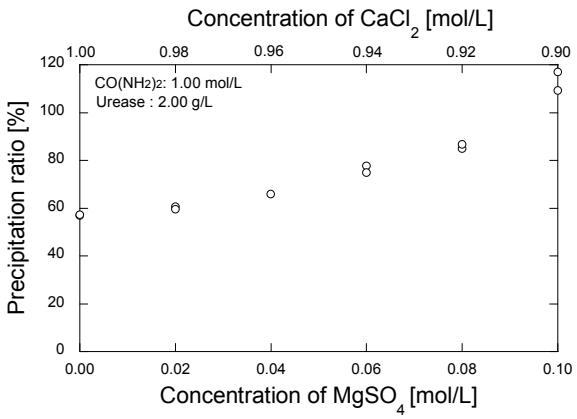

Figure 4. Precipitated mass in various concentrations of $MgSO_4$-$CaCl_2$.

XRD and SEM analyses were conducted to evaluate the effect of magnesium on the mineralogy and morphology of precipitated materials. The XRD results in Figure 5 show the impact of magnesium on the crystalline material. In A0, without magnesium, the main material was calcite and the low peaks of aragonite (i.e., d = 3.392, 3.182, and 2.705) were also found. In addition, the other calcium carbonate polymorph of vaterite may also be generated during the precipitation process. As aforementioned, the XRD patterns of aragonite and vaterite are very similar, and may partially overlap. Therefore, the presence of vaterite cannot completely be excluded because of the variety of vaterite structures. However, vaterite may not be able to exist as a distinct structure [34] and, thus, the distinct peaks obtained from the analyses (Figure 5) are most likely to be aragonite. In A1, when 0.02 mol/L of magnesium sulfate was added to the grouting solution, the peak of aragonite significantly increased and, in contrast, the peak of calcite decreased. The peaks of gypsum (i.e., d = 7.63 and 4.283) were also found in addition to that of calcite and aragonite. The peaks of calcite were found to be approximately constant when the range in substituted magnesium sulfate was 0.04–0.10 mol/L. As the concentration of magnesium sulfate was increased, the peaks of gypsum gradually increased. The results of mineralogical analysis revealed that the precipitated materials were composed of calcite, aragonite, and gypsum.

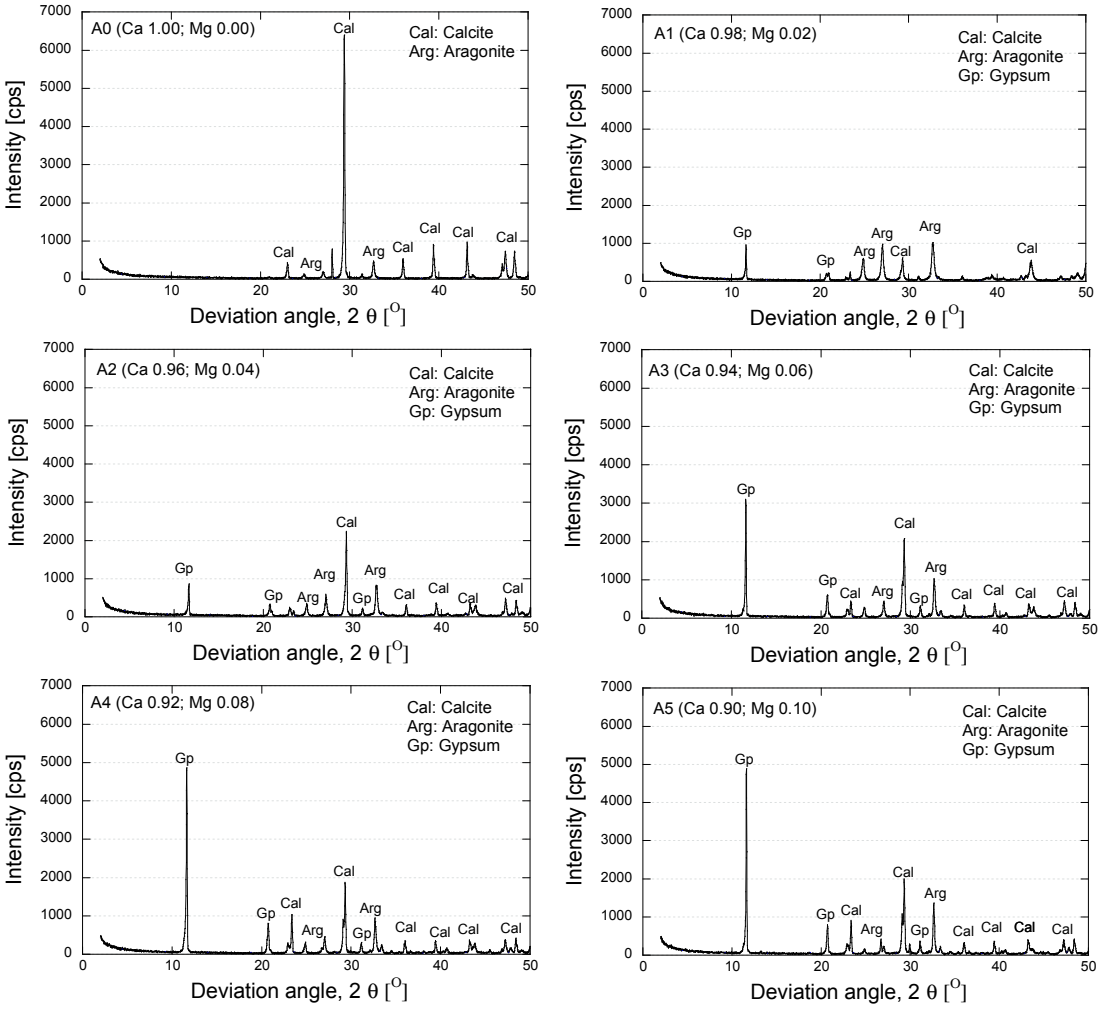

Figure 5. X-ray diffraction results of precipitated materials.

The XRD quantitative analysis was used to determine the composition of the precipitated materials [31–33]. The calibration curve was developed by mixing a pure and internal material

with the ratios of 0%–100%, 10%–90%, 30%–70%, 50%–50%, 70%–30%, 90%–10%, and 100%–0%, respectively. Validation data were also produced to eliminate any errors that might occur due to the process, e.g., sample preparation. Quartz (SiO_2) which has clearly different peaks from those of the precipitated materials, was selected as the internal standard material in this work. Calcite and gypsum, with claimed purity levels greater than 95.0% from the Kanto Chemicals Co., Inc., Tokyo, Japan and aragonite red C, from Sefrou, Marocco, were used as the pure materials. The XRD results for quartz, calcite, aragonite, and gypsum are shown in Figure 6.

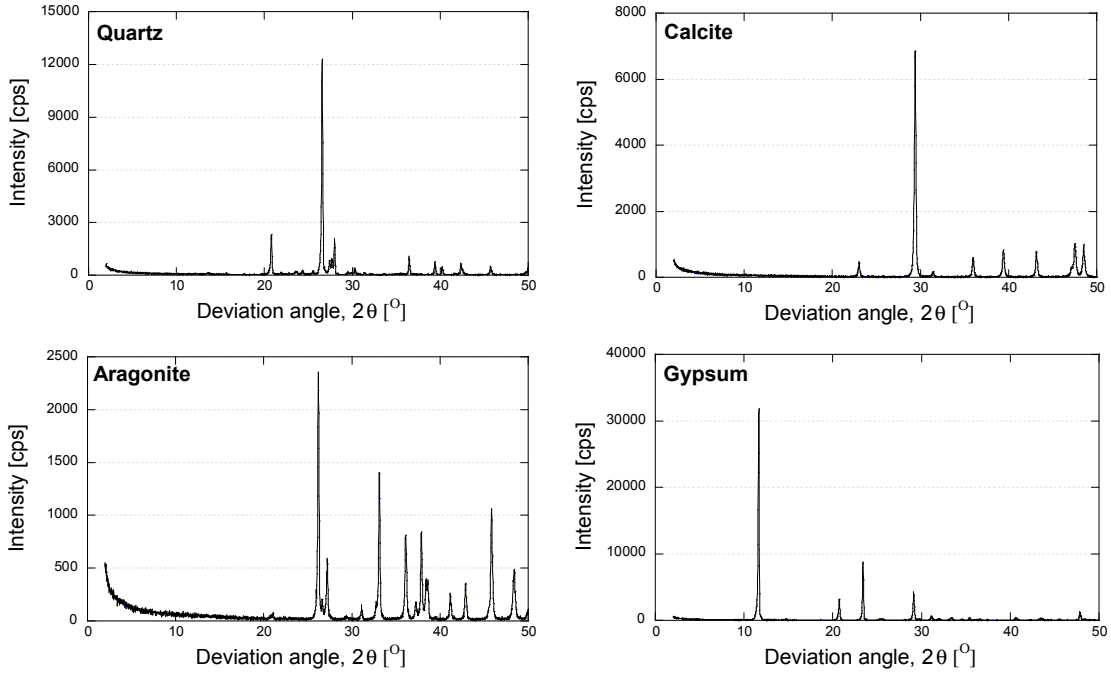

Figure 6. X-ray diffraction results of internal standard and pure minerals.

Various combinations of masses of calcite (Cal)–SiO_2, aragonite (Arg)–SiO_2, and gypsum (Gp)–SiO_2 were evaluated under the same terms. Two sets of combinations of Cal–Arg–Gp were also assessed to validate the results of the quantitative analysis. The experimental conditions for the quantitative analysis are shown in Table 2.

Table 2. Experimental conditions for calibration curve of quantitative analysis.

Case	Material Mass (%) *			
	Pure Material			Internal Standard Material
	Cal	Arg	Gp	SiO_2
1	0	0	0	100
2	10	10	10	90
3	30	30	30	70
4	50	50	50	50
5	70	70	70	30
6	90	90	90	10
7	100	100	100	0
Val 1	40	40	20	-
Val 2	30	30	40	-

* In a total mass of 0.10 g.

The relation between the intensity and the percentage mass of the pure materials is shown in Figure 7. In two experiments (i.e., Val 1 and Val 2), the data were examined to validate the calibration curve. The maximum percentage error was found to be 4%.

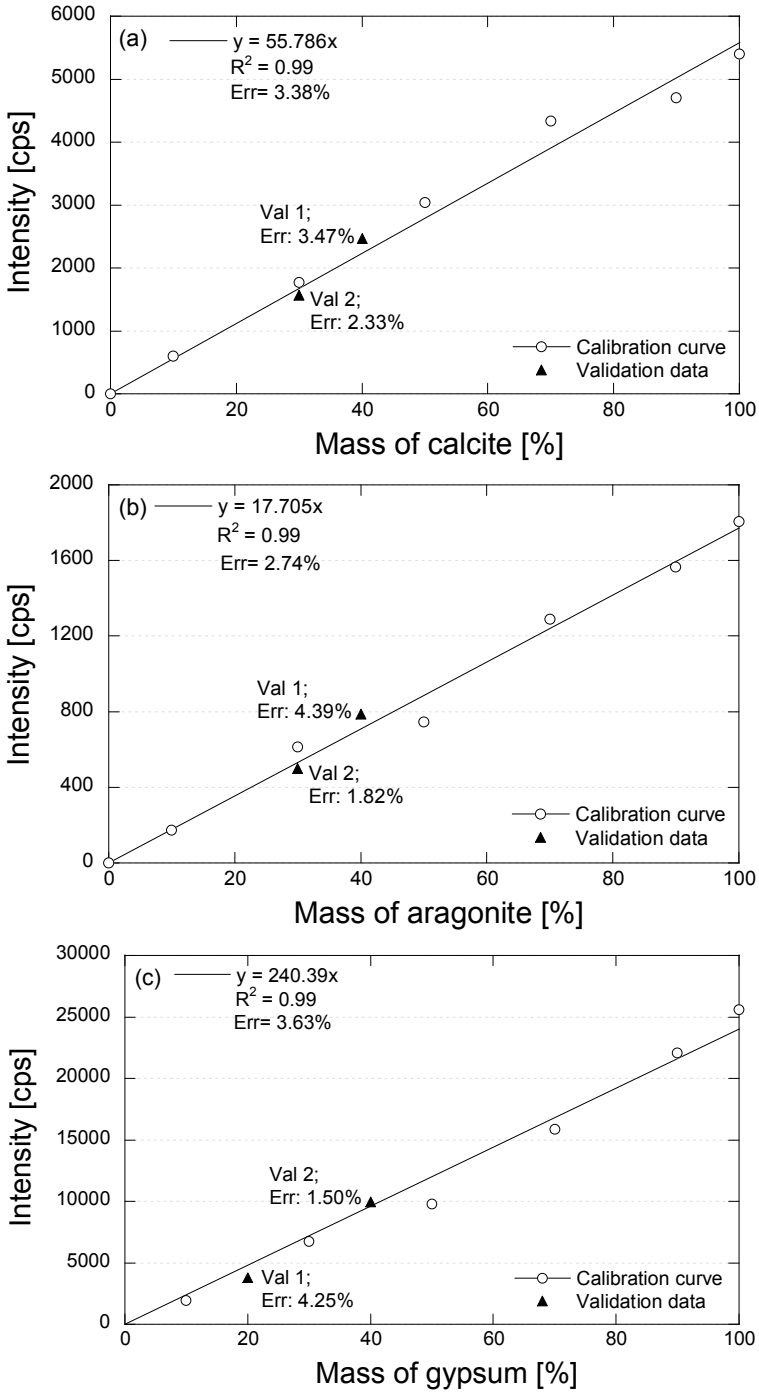

Figure 7. Calibration curve for XRD quantitative analysis: (**a**) calcite; (**b**) aragonite; and (**c**) gypsum.

The compositions of the precipitated materials were examined by plotting the intensity of the main peaks of calcite, aragonite, and gypsum on the calibration curves, and the mass percentage was obtained. Table 3 shows the mineral compositions of the precipitated materials and its summaries are depicted in Figure 8. The total amount of precipitated materials is seen to gradually increase after the substitution of magnesium sulfate. In the case of A0, which is without magnesium, mostly

calcite (i.e., 96.4%) was found as the precipitated material. In the case of A1, when 0.02 mol/L of magnesium was added, a significant amount of aragonite was formed; a mass percentage of aragonite of 66.75% was obtained in addition to that of calcite of 26.15%. Moreover, a mass percentage of gypsum of 7.10% was also formed. Furthermore, the mass percentage of gypsum increased as the concentration of magnesium sulfate was further increased. The results indicated that the substitution of low concentrations of magnesium sulfate (i.e., 0.02 and 0.04 mol/L) significantly promoted the formation of aragonite in the precipitation process. The presence of a low concentration of magnesium sulfate might allow the magnesium ion to delay the reaction rate and promote the formation of aragonite. In contrast, the substitutions of 0.06–0.10 mol/L magnesium sulfate might enhance the reaction rate and promote the formation of gypsum.

Table 3. Amount and composition of precipitated materials.

Case	Concentration of $CaCl_2$ (molŁ)	Concentration of $MgSO_4$ (molŁ)	Total Precipitated Mass (g) *	Mineral Composition					
				Calcite		Aragonite		Gypsum	
				(g)	(%)	(g)	(%)	(g)	(%)
A0	1.00	0.00	1.71	1.65	96.67	0.06	3.33	0.00	0.00
			1.72	1.65	96.13	0.07	3.87	0.00	0.00
A1	0.98	0.02	1.82	0.48	26.58	1.19	65.30	0.15	8.12
			1.79	0.46	25.72	1.22	68.21	0.11	6.07
A2	0.96	0.04	1.98	1.39	70.38	0.48	24.46	0.10	5.14
			1.98	1.41	71.00	0.47	23.64	0.11	5.32
A3	0.94	0.06	2.33	1.41	60.36	0.46	19.72	0.46	19.67
			2.25	1.47	65.30	0.45	20.15	0.33	14.55
A4	0.92	0.08	2.55	1.31	51.29	0.49	19.21	0.75	29.50
			2.60	1.26	48.61	0.59	22.64	0.75	28.75
A5	0.90	0.10	3.28	1.91	58.13	0.30	9.19	1.07	32.68
			3.51	1.99	56.57	0.28	8.08	1.25	35.35

* In 30 mL of grout solution.

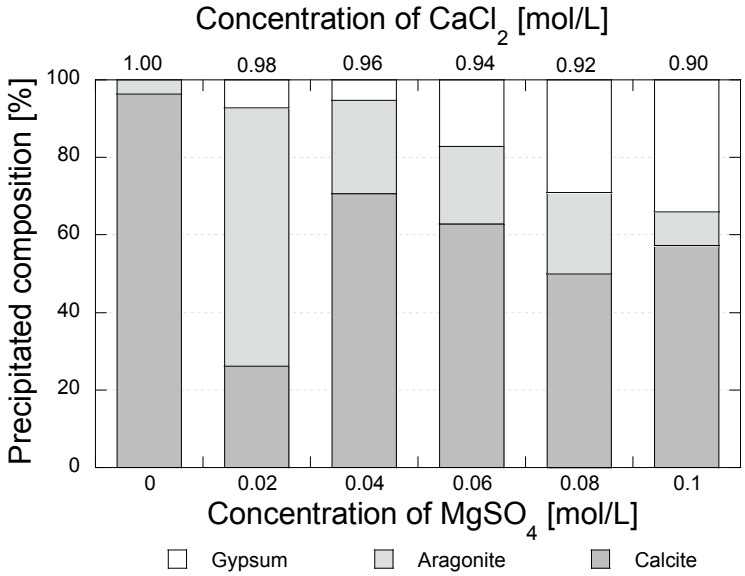

Figure 8. Composition of precipitated materials.

The evolutions of the crystal phase observed by SEM are shown in Figure 9. In A0, which is the crystal structure image of the precipitated materials without the substitution of magnesium sulfate, rhombohedral calcite was formed. As the magnesium sulfate was substituted, the structure phase

changed, and new crystals of aragonite and gypsum were also formed. The phase of aragonite clearly appeared in A1 and A2, when 0.02–0.04 mol/L of magnesium was added, respectively. Gypsum clearly formed when magnesium with concentrations of >0.06 mol/L (i.e., A3, A4, and A5) were added. The agglomeration phase of the precipitated materials was also formed by the substitution of magnesium. The SEM results confirmed that magnesium sulfate could be utilized to promote the formation of aragonite and gypsum in addition to calcite.

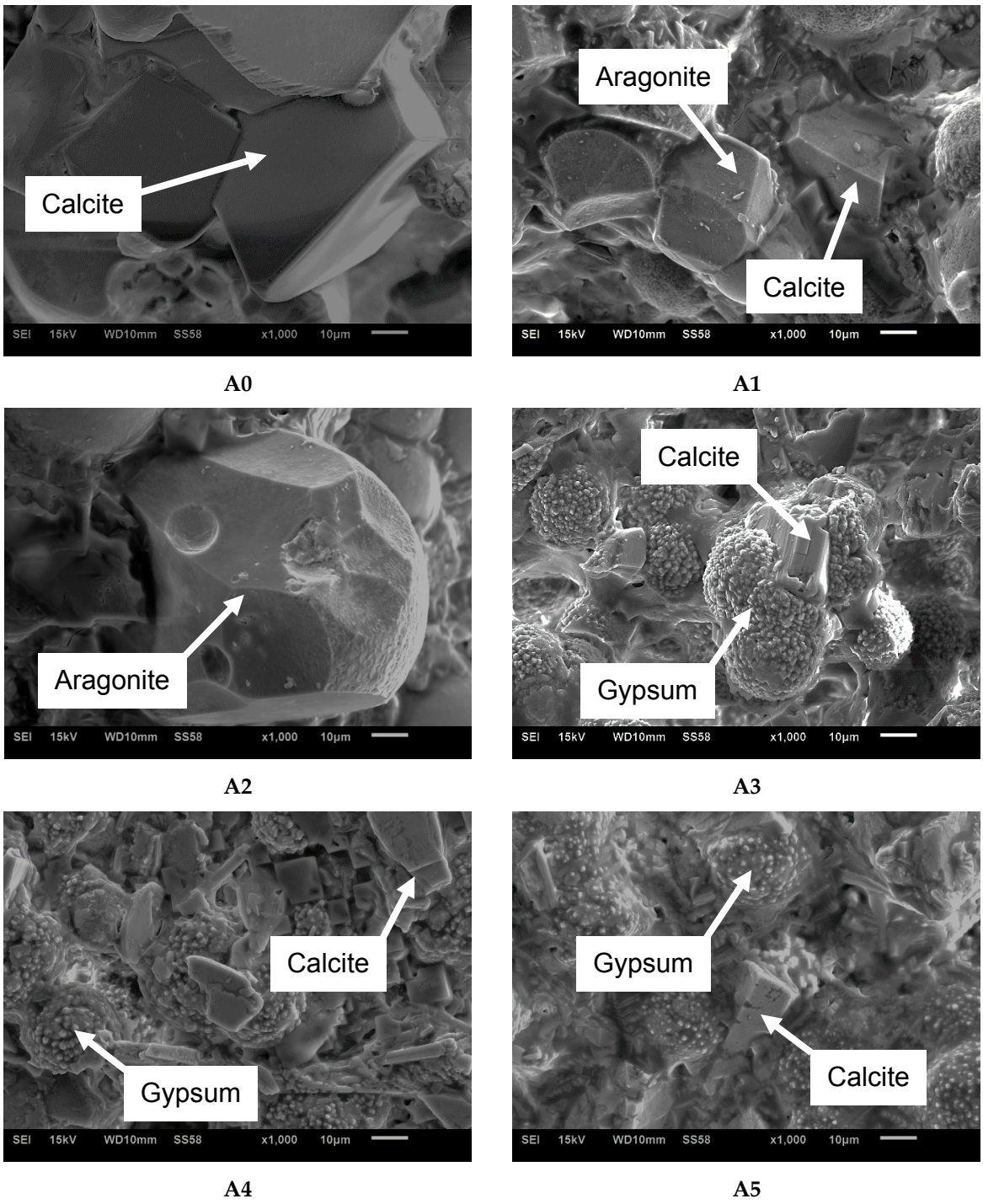

Figure 9. Scanning electron microscopy of precipitated minerals.

In order to evaluate the effect of the presence of aragonite and gypsum, as the precipitated materials on the mechanical properties of treated sand, A0, A1, A2, and A5 were selected as the grouting solutions. A0, which may produce mostly calcite, A1 and A2, which may produce mostly aragonite-calcite, and A5, which may produce mostly calcite-gypsum, were injected into the sand samples. Then, the effects of the presence of aragonite and gypsum in the EMCP technique were examined through UCS tests. By comparing all of the cases with those obtained from the literature, the effectiveness of aragonite and gypsum in the EMCP technique was evaluated. The experimental conditions for the PVC cylinder tests are listed in Table 4.

Table 4. Experimental conditions for PVC cylinder tests.

Case	Grouting Solution	Conc. of Urease (g/L)	Reagent Compositions		
			Conc. of Urea (molŁ)	Conc. of $CaCl_2$ (molŁ)	Conc. of $MgSO_4$ (molŁ)
U_1	A0	2.00	1.00	1.00	0.00
U_2	A1	2.00	1.00	0.98	0.02
U_3	A2	2.00	1.00	0.96	0.04
U_4	A5	2.00	1.00	0.90	0.10

In order to evaluate the amount of precipitated material within the sand sample, the acid leaching method with a percentage error of 1.8% was conducted [4]. In this process, the treated sample was washed with distilled water to dissolve the salt materials and then dried at a temperature of 100 °C for 24 h. The dried samples were weighed and washed with 0.1 mol/L of HCl several times until air bubbles no longer appeared. Filter paper (PS of 11 μm) was utilized to minimize the lost mass of sand during the washing process. The sample was dried again, and the final weight was taken. The dry weight lost during the acid leaching was examined and assumed to be the weight of the precipitated materials [4,9,13]. The reactions taking place are expressed by Equations (8) and (9):

$$CaCO_3 + 2HCl \rightarrow CaCl_2 + CO_2 + H_2O \quad (8)$$

$$CaSO_4 + 2HCl \rightarrow CaCl_2 + H_2SO_4 \quad (9)$$

The results of the PVC cylinder tests are depicted in Figure 10. The mass of the precipitated materials, varying in the range of 4%–10% of the soil mass, was obtained by 1–3 PV injections (Figure 10a). The precipitated mass within the treated sand increased as the number of injections was further increased. When one pore volume (PV) of grouting solution was injected, a lower precipitated mass was obtained for U_1 than for U_2, U_3, and U_4. The precipitated mass increased as the number of injections was increased. However, the obtained mineral mass in the case of U_4 was found lower than the other cases (Figure 10a). The maximum strength of 0.6 MPa was achieved in the presence a 10% mineral precipitation in U_2 and U_3. The UCS of the treated sand improved 2.5-fold compared to that without magnesium (i.e., U_1). In the case of U_4, a lower mass of precipitated materials was formed with the same number of injections. The presence of a high concentration of magnesium sulfate might promote the formation of gypsum and enhance the reaction rate. The precipitate was formed before all of the grouting solution flowed through the sample and, hence, a higher amount of precipitated minerals was formed close to the surface. The maximum precipitated mass of 8%, which corresponds to the strength of 0.2 MPa (Figure 10b), was obtained. The presence of a high concentration of magnesium sulfate in the grouting solution enhanced the reaction rate. The precipitation process occurred quickly after mixing, and the precipitated materials might have formed before all of the solution had been passed through the sand samples. The precipitated materials were concentrated in the upper side of the sand samples. This may have hampered the permeation of the injecting solution between the soil particles and, hence, the number of injections was limited. However, the mineralogical analyses of the treated sand were not conducted, so the exact composition of the precipitated materials

cannot be identified. In comparison to the previous study, in which the calcite precipitation technique was performed without magnesium [7], the maximum strength obtained in this study was roughly 40% higher for the same mineral mass. The combination of calcite-aragonite (i.e., U_2 and U_3) as the precipitated minerals brought about a significant improvement in the strength of the treated sand. The results indicated that the substitution of a low concentration of magnesium sulfate into the injecting solution in the EMCP technique has the potential to improve the strength of the treated sand.

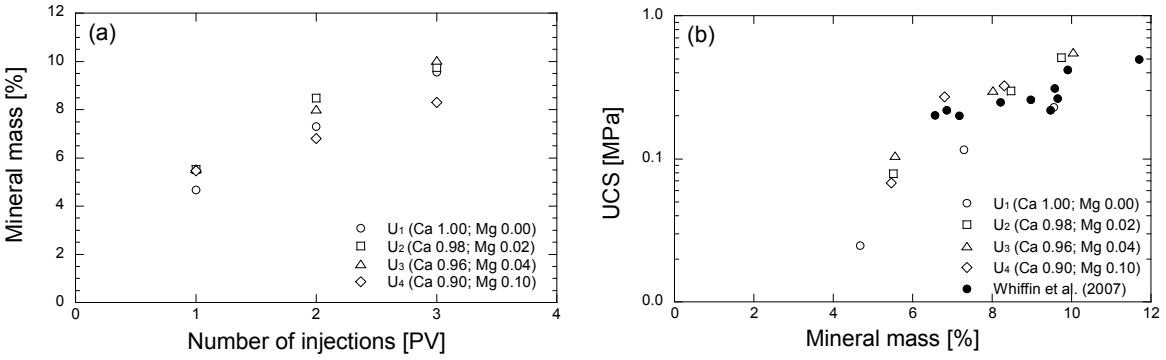

Figure 10. Results of PVC cylinder tests: (**a**) mineral mass in various number of injections; and (**b**) relation between mineral mass and UCS.

4. Conclusions

The applicability of magnesium sulfate as the substituted material in enzyme-mediated calcite precipitation (EMCP) has been evaluated for its possible application as a soil-improvement technique. The effects of the addition of magnesium sulfate on the amount and the mineralogical substance of the precipitated materials have been assessed. The evolution of the mechanical properties of treated sand was also evaluated through unconfined compressive strength (UCS) tests. The precipitated mass was seen to increase as the concentration of magnesium sulfate was increased. The mineralogical analysis revealed that the substitution of magnesium sulfate into the injecting solution composed of urea, urease, and $CaCl_2$ was a potential method for promoting the formation of aragonite and gypsum. Especially, the low concentrations of magnesium sulfate (i.e., 0.02 and 0.04 mol/L) significantly promoted the formation of aragonite. Furthermore, a large amount of gypsum was formed when 0.10 mol/L of magnesium sulfate was substituted.

The UCS test results showed that besides calcite, the presence of aragonite as a precipitated mineral resulted in greater improvement in the strength of the treated sand than the sand treated purely by calcite. A maximum strength of 0.6 MPa was obtained from the treated samples in the presence of a mineral mass of 10%. In comparison to the previous studies, which addressed calcite precipitation only, the obtained strength in this study was higher for the same precipitated mass. The results of this study have elucidated that the application of magnesium sulfate to the EMCP technique may be an alternative soil-improvement method.

Acknowledgments: This work has been partly supported by a research grant from the Penta-Ocean Constructions Co., Ltd. and BU Kemendikbud, Ministry of Education and Culture of Indonesia. Their support is gratefully acknowledged.

Author Contributions: Heriansyah Putra has performed all the experiments and analyzed the data; Hideaki Yasuhara has supervised this work, partly conducted the experiments and analyzed the data; Naoki Kinoshita has suggested how to proceed this work and partly conducted the experiments; Akira Hirata has suggested how to conduct the experiments and analysed the data.

Conflicts of Interest: The authors declare no conflict of interest.

References

1. Neupane, D.; Yasuhara, H.; Kinoshita, N. Evaluation of enzyme mediated calcite grouting as a possible soil improvement technique. In *Computer Method and Recent Advances in Geomechanics*; Oka, F., Murakami, A., Uzuoka, R., Kimoto, S., Eds.; CRC Press: Boca Raton, FL, USA, 2015; pp. 1169–1172.
2. Neupane, D.; Yasuhara, H.; Kinoshita, N.; Putra, H. Distribution of grout material within 1-m sand column in insitu calcite precipitation technique. *Soil Found.* **2015**, *55*, 1512–1518. [CrossRef]
3. Neupane, D.; Yasuhara, H.; Kinoshita, N.; Ando, Y. Distribution of mineralized carbonate and its quanti fi cation method in enzyme mediated calcite precipitation technique. *Soil Found.* **2015**, *55*, 447–457. [CrossRef]
4. Putra, H.; Yasuhara, H.; Kinoshita, N.; Neupane, D.; Lu, C.-W. Effect of Magnesium as Substitute Material in Enzyme-Mediated Calcite Precipitation for Soil-Improvement Technique. *Front. Bioeng. Biotechnol.* **2016**, *4*, 37. [CrossRef] [PubMed]
5. Van Paassen, L.A.; Daza, C.M.; Staal, M.; Sorokin, D.Y.; van der Zon, W.; van Loosdrecht, M.C.M. Potential soil reinforcement by biological denitrification. *Ecol. Eng.* **2010**, *36*, 168–175. [CrossRef]
6. Cheng, L.; Cord-Ruwisch, R.; Shahin, M.A. Cementation of sand soil by microbially induced calcite precipitation at various degrees of saturation. *Can. Geotech. J.* **2013**, *50*, 81–90. [CrossRef]
7. Whiffin, V.S.; van Paassen, L.A.; Harkes, M.P. Microbial Carbonate Precipitation as a Soil Improvement Technique. *Geomicrobiol. J.* **2007**, *24*, 417–423. [CrossRef]
8. Harkes, M.P.; van Paassen, L.A.; Booster, J.L.; Whiffin, V.S.; van Loosdrecht, M.C.M. Fixation and distribution of bacterial activity in sand to induce carbonate precipitation for ground reinforcement. *Ecol. Eng.* **2010**, *36*, 112–117. [CrossRef]
9. Yasuhara, H.; Neupane, D.; Hayashi, K.; Okamura, M. Experiments and predictions of physical properties of sand cemented by enzymatically-induced carbonate precipitation. *Soil Found.* **2012**, *52*, 539–549. [CrossRef]
10. Putra, H.; Yasuhara, H.; Kinoshita, N.; Neupane, D. Optimization of Calcite Precipitation as a Soil Improvement Technique. In Proceedings of the 2nd Makassar International Conference on Civil Engineering, Makassar, Indonesia, 11–12 August 2015; pp. 9–14.
11. Martinez, B.C.; DeJong, J.T.; Ginn, T.R.; Montoya, B.M.; Barkouki, T.H.; Hunt, C.; Tanyu, B.; Major, D. Experimental Optimization of Microbial-Induced Carbonate Precipitation for Soil Improvement. *J. Geotech. Geoenviron. Eng.* **2013**, *139*, 587–598. [CrossRef]
12. DeJong, J.T.; Fritzges, M.B.; Nüsslein, K. Microbially Induced Cementation to Control Sand Response to Undrained Shear. *J. Geotech. Geoenviron. Eng.* **2006**, *132*, 1381–1392. [CrossRef]
13. Neupane, D.; Yasuhara, H.; Kinoshita, N.; Unno, T. Applicability of Enzymatic Calcium Carbonate Precipitation as a Soil-Strengthening Technique. *J. Geotech. Geoenviron. Eng.* **2013**, *139*, 2201–2211. [CrossRef]
14. Nemati, M.; Greene, E.A.; Voordouw, G. Permeability profile modification using bacterially formed calcium carbonate: Comparison with enzymic option. *Process Biochem.* **2005**, *40*, 925–933. [CrossRef]
15. Yasuhara, H.; Hayashi, K.; Okamura, M. Evolution in Mechanical and Hydraulic Properties of Calcite-Cemented Sand Mediated by Biocatalyst. In *Geo-Frontiers 2011: Advances in Geotechnical Engineering*; ASCE: Reston, VA, USA, 2011; pp. 3984–3992.
16. Van Paassen, L.A.; Ghose, R.; van der Linden, T.J.M.; van der Star, W.R.L.; van Loosdrecht, M.C.M. Quantifying Biomediated Ground Improvement by Ureolysis: Large-Scale Biogrout Experiment. *J. Geotech. Geoenviron. Eng.* **2010**, *136*, 1721–1728. [CrossRef]
17. De Muynck, W.; de Belie, N.; Verstraete, W. Microbial carbonate precipitation in construction materials: A review. *Ecol. Eng.* **2010**, *36*, 118–136. [CrossRef]
18. Okwadha, G.D.O.; Li, J. Optimum conditions for microbial carbonate precipitation. *Chemosphere* **2010**, *81*, 1143–1148. [CrossRef] [PubMed]
19. Boyd, V.H. The Effect of Calcium and Magnesium on Carbonate Mineral Precipitation during Reactive Transport in a Model Subsurface Pore Structure. Ph.D. Thesis, University of Illinois, Champaign, IL, USA, 2012.
20. Park, W.K.; Ko, S.-J.; Lee, S.W.; Cho, K.-H.; Ahn, J.-W.; Han, C. Effects of magnesium chloride and organic addictives on synthesis of aragonite precipitated calcium carbonate. *J. Cryst. Growth* **2008**, *310*, 2593–2601. [CrossRef]
21. Litvin, A.L.; Valiyaveettil, S.; Kaplan, D.L.; Mann, S. Template-Directed Synthesis of Aragonite Under Supramolecular Hydrogen-Bonded Langmuir Monolayers. *Adv. Mater.* **1997**, *9*, 124–127. [CrossRef]

22. "Aragonite." A Dictionary of Earth Sciences. Encyclopedia.com. Available online: http://www.encyclopedia.com/science/dictionaries-thesauruses-pictures-and-press-releases/aragonite (accessed on 1 November 2016).
23. "Calcite." A Dictionary of Earth Sciences. Encyclopedia.com. Available online: http://www.encyclopedia.com/science/dictionaries-thesauruses-pictures-and-press-releases/calcite (accessed on 1 November 2016).
24. Friedman, G.; Schultz, D. Precipitation of vaterite ($CaCO_3$) during oil field drilling. *Mineral. Mag.* **1994**, *58*, 401–408. [CrossRef]
25. Kahmi, S.R. On the structure of vaterite, $CaCO_3$. *Acta Crystallogr.* **1963**, *16*, 770–772.
26. Wang, J.; Becker, U. Structure and carbonate orientation of vaterite ($CaCO_3$). *Am. Mineral.* **2009**, *94*, 380–386. [CrossRef]
27. De Villiers, J.P.R. Crystal structures of aragonite, strontianite, and witherite. *Am. Mineral.* **1971**, *56*, 758–767.
28. Dal Negro, A.; Ungaretti, L. Refinement of the Crystal Structure of Aragonite. *Am. Mineral.* **1971**, *56*, 768–772.
29. ASTM International. *International, Standard Practice for Classification of Soils for Engineering Purposes (Unified Soil Classification System)*; ASTM Standard Guide. D5521-5; ASTM: West Conshohocken, PA, USA, 2000.
30. Yasuhara, H.; Neupane, D.; Kinosita, N.; Hayashi, K.; Unno, T. Solidification of sand soils induced by calcium carbonate precipitation utilizing biocatalyst. *J. Jpn. Soc. Civ. Eng. Ser. C Geosph. Eng.* **2014**, *70*, 290–300. [CrossRef]
31. Chung, F.H. Quantitative interpretation of X-ray diffraction patterns of mixtures. III. Simultaneous determination of a set of reference intensities. *J. Appl. Crystallogr.* **1975**, *8*, 17–19. [CrossRef]
32. Chipera, S.J.; Bish, D.L. Fitting Full X-Ray Diffraction Patterns for Quantitative Analysis: A Method for Readily Quantifying Crystalline and Disordered Phases. *Adv. Mater. Phys. Chem.* **2013**, *3*, 47–53. [CrossRef]
33. Connolly, J.R. *Introduction Quantitative X-ray Diffraction Methods. Fundamentals of X-ray Powder Diffraction*; Nuevo Mexico University: Albuquerque, NM, USA, 2012.
34. Demichelis, R.; Raiteri, P.; Gale, J.D.; Dovesi, R. The multiple structures of vaterite. *Cryst. Growth Des.* **2013**, *13*, 2247–2251. [CrossRef]